High-Pressure Study on Intramolecular Excimer Formation of 1,3-Di-1-pyrenylpropane in Various Solvents

Kimihiko Hara* and Hiroyuki Yano

Contribution from the Department of Chemistry, Faculty of Science, Kyoto University, Sakyo-ku, Kyoto 606, Japan. *Received March 30, 1987*

Abstract: We have examined the viscosity effects of intramolecular excimer (IE) formation in 1,3-di-1-pyrenylpropane (DPP) at high pressures in various solvents. The formation is strongly and exclusively dependent on solvent viscosity, while it is insensitive to solvent polarity. The rates of the excimer formation estimated from fluorescence quantum yields are represented as a unique function of solvent viscosity. A hindered rotation model based on Kramers' theory was applied successfully. The more general results without specific interaction of solvent were obtained. The intrinsic activation energy (15-18 kJ/mol), the intrinsic activation volume (-2.5 cm^3/mol), and the frequency for the top of the barrier of this IE formation were determined.

Formation processes involving large-amplitude motion, such as intramolecular excimer (IE) formation in bichromophoric molecules in which bulky chromophores must twist with respect to the connecting bonds, should depend on the frictional forces exerted by solvents. For full understanding of these solvent effects, there are further questions to be answered. The first is whether the rates of formation are controlled exclusively by the viscosity of solvents; namely, whether the rates are equal at the same viscosity, independent of the means by which that viscosity value was produced, i.e., by changing the pressure, the temperature, or the solvent. The second is the question of what type of analytical formulation is possible for the viscosity dependence of the IE formation process and what type of model is applicable for describing the microscopic motions involved in the IE formation.

We found in some bichromophoric compounds that the formation rates of their intramolecular excited states are really dependent on solvent viscosity.[1-4] As for the IE formation of 1,3-di-1-pyrenylpropane (DPP), Thistlethwaite et al.[5] reported that it was not dependent on solvent viscosity, while Zachariasse et al.[6] argued against it. Thereafter, Offen et al.[7] reported a viscosity dependence that is inversely proportional to solvent viscosity, indicating a diffusion-controlled collision process. In our previous paper, we suggested from the study at high pressures[8] that this formation is absolutely dependent on solvent viscosity and proposed that the hydrodynamic model of hindered rotation based on Kramers' theory may be applicable to the viscosity dependence.

In most studies on the influence of solvent viscosity, a series of homologous solvents[9,10] or mixed solvents[11-14] have been used to achieve viscosity variation. A possible problem in these approaches is that there may exist large local variations in the solvent shell interactions with the aromatic chromophores. Specific and/or steric interactions between solvent molecules and aromatic chromophores should affect the rotational transformation process and the stability of the excimer. The application of high hydrostatic pressure, on the other hand, makes it possible to minimize this problem. It achieves a large amount of continuous variation in viscosity without changing the chemical character of solvent shell.

In this paper we report the results of a more detailed study of the viscosity dependence of the IE formation of DPP by examining over the wide range of viscosity (more than 2 orders of magnitude) the effects of the application of high hydrostatic pressures in various solvents.

Experimental Section

DPP was synthesized by using the methods as described in the literature.[15] An authentic sample was also obtained from Molecular Probes, Inc. No impurity was detectable by TLC or in the absorption and emission spectra. Except for 2,6,10,14-tetramethylpentadecane (TMPD), the solvents used were spectroscopic grade quality, and they were used as received. TMPD was obtained from the middle cut of two successive vacuum distillations after dehydration. This cut showed no emission in the spectral region of interest at the sensitivity levels used. The concentration of DPP was less than 5.0×10^{-5} mol/L, in which intermolecular contributions vanish. All solutions were degassed by repeated freeze-pump-thaw cycles just before measurement.

The high-pressure cell, emission equipment, and methods of data processing have been described elsewhere.[1,16] Measurements at high pressures were carried out at 303 K. Temperature was controlled by circulating temperature-controlled water into a cell jacket. Temperature control of the quartz Dewar, which was used for measurements at normal pressure, was accomplished with a coolant that was passed through liquid nitrogen and then heated to the appropriate temperature. It was regulated to ±0.5 °C at each temperature. Fluorescence spectra were recorded by using excitation at 334.1 nm. The ratios of the quantum yields from the IE state (ϕ_{IE}) and from the locally excited (LE) state (ϕ_{LE}) and their peak energies were determined.

Results and Discussion

Peak Shifts with Pressure. The peak locations of the LE and IE bands at normal pressure ($\bar{\nu}_{max}$) and their peak shifts with pressure ($d\bar{\nu}_{max}/dP$) in the different solvents studied are listed in Table I together with the viscosities at normal pressure (η_0) and the polarity parameters (Δf). The peak maximum of the LE band is assigned as a $0 \rightarrow 0$ transition of the pyrenyl chromophore. In high viscosity solvents, such as glycerol (612 cP), the yield of the IE emission becomes too small to be detected. It is evident from Table I that the IE band as well as the LE band is not affected by solvent polarity. This suggests that their excited dipole moments are not so different from those of the ground state.

The peak shifts with pressure were determined from the initial slopes after fitting to polynomials. Both bands shifted to the red with pressure. The LE band changes linearly, while the IE band saturates as pressure increases, which is shown in Figure 1 for *n*-hexane as a representative profile. The amount of peak shift with pressure for each state is almost equal among the solvents with different polarities. The small rate of red-shift for the LE band with pressure, $d\bar{\nu}_{max}/dP = -9$ to -16 cm^{-1}/kbar, indicates that this emission can be assigned as an $^1L_b \rightarrow {}^1A$ transition.[17]

(1) Hara, K.; Arase, T.; Osugi, J. *J. Am. Chem. Soc.* **1984**, *106*, 1968.
(2) Hara, K.; Arase, T. *Chem. Phys. Lett.* **1984**, *107*, 178.
(3) Hara, K.; Obara, K. *Chem. Phys. Lett.* **1985**, *117*, 96.
(4) Hara, K. *Physica B+C (Amsterdam)* **1986**, *139 & 140B*, 705.
(5) Snare, M. J.; Thistlethwaite, P. J.; Ghiggino, K. P. *J. Am. Chem. Soc.* **1983**, *105*, 3328.
(6) Zachariasse, K. A.; Duveneck, G.; Busse, R. *J. Am. Chem. Soc.* **1984**, *106*, 1045.
(7) Turley, W. D.; Offen, H. W. *J. Phys. Chem.* **1985**, *89*, 2933.
(8) Hara, K.; Yano, H. *J. Phys. Chem.* **1986**, *90*, 4265.
(9) Johnson, G. E. *J. Chem. Phys.* **1975**, *63*, 4047.
(10) Velsko, S. P.; Waldeck, D. H.; Fleming, G. R. *J. Chem. Phys.* **1983**, *78*, 249.
(11) Avouris, P.; Kordas, J.; El-Bayoumi, M. A. *Chem. Phys. Lett.* **1974**, *26*, 373.
(12) Wang, Y. C.; Morawetz, H. *J. Am. Chem. Soc.* **1976**, *98*, 3611.
(13) Goldenberg, M.; Emert, J.; Morawetz, H. *J. Am. Chem. Soc.* **1978**, *100*, 7171.
(14) Liao, T.-P.; Okamoto, Y.; Morawetz, H. *Macromolecules* **1979**, *12*, 535.
(15) Zachariasse, K. A.; Kühnle, W. *Z. Phys. Chem. (Munich)* **1976**, *101*, 267.
(16) Hara, K.; Katou, Y.; Osugi, J. *Bull. Chem. Soc. Jpn.* **1983**, *56*, 1308.

0002-7863/88/1510-1911$01.50/0

Table I. Solvent Viscosity, Solvent Polarity Parameter, Peak Energy, and Peak Shift with Pressure

solvent	viscosity at 1 bar, cP	polarity parameter[a]	peak energy at 1 bar, 10^3 cm^{-1}		peak shift with pressure, cm^{-1}/kbar	
			LE	IE	LE	IE
acetone	0.293	0.285	26.58	20.16	−12	−134
n-hexane	0.296	0.000	26.62	20.25	−12	−170
methylcyclohexane	0.627		26.57	20.20	−12	−163
ethanol	1.00	0.289	26.58	20.16	−9	−148
isobutyl alcohol	2.913	0.266	26.61	20.17	−10	−136
TMPD	4.4		26.59	20.19	−16	−84
glycerol	612		26.54			

[a]Solvent polarity parameter: $\Delta f = (\epsilon - 1)/(2\epsilon + 1) - (n^2 - 1)/(2n^2 + 1)$ at 25 °C.

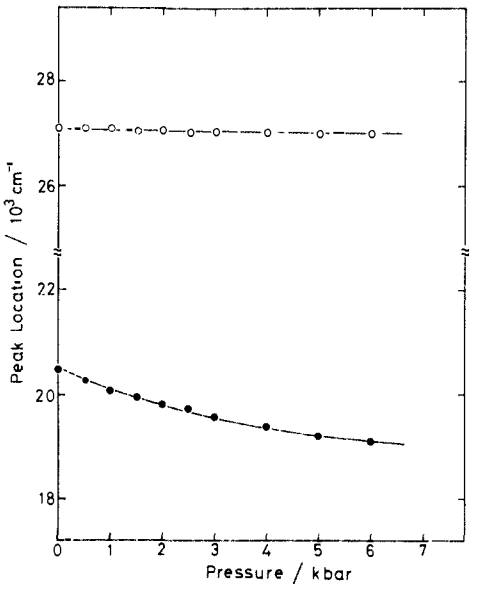

Figure 1. Shift in the peak energies of the LE state (○) and IE state (●) of DPP with pressure in *n*-hexane.

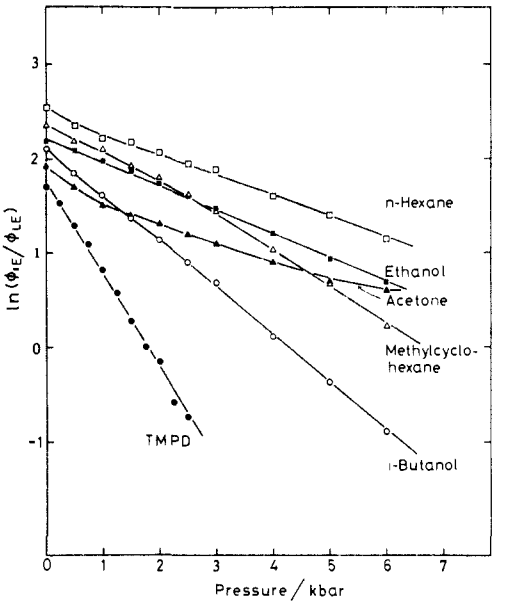

Figure 2. Pressure dependence of the quantum yield ratio in various solvents at 303 K.

In the case of $^1L_a \rightarrow {}^1A$ transition, it is a few times larger in polar solvents.[17]

On the other hand, the pressure shift of the IE band is $d\bar{\nu}_{max}/dP = -84$ to -170 cm^{-1}/kbar, which is larger than that of the LE band by 1 order of magnitude. Another type of excited state, which exhibits excimerlike emission, is the so-called "twisted intramolecular charge transfer" (TICT) state.[18] The amount of the shift is more than -300 cm^{-1}/kbar for *p*-9-anthryl-*N*,*N*-dimethylaniline (ADMA) and 4-(9-anthrylmethyl)-*N*,*N*-dimethylaniline (AMDMA),[19] -220 cm^{-1}/kbar for 9,9′-bianthryl (BA),[1] and -208 cm^{-1}/kbar for 4-(dimethylamino)benzonitrile (DMABN).[19] We found that the amount of the shift for the IE band of DPP is approximately half of the TICT state. By further detailed analysis of the energy shift with pressure, we will surely find it a more useful and definite measure to determine the nature of fluorescent electronic states.

Scheme of the IE Formation. Thistlethwaite et al.[5] reported a scheme for IE formation with DPP, consisting essentially of two simultaneously operating but noninteracting subschemes that are each identical with the schemes that describe intermolecular excimer formation.[20] In contrast, Zachariasse et al.[6] proposed that a more general scheme of two interacting monomers or excimers may be possible. In the present study, we have no such indication of the two-excimer scheme in the spectra as well as in the Arrhenius plots. In any case, however, the major part of the excimer is formed through the subscheme with the smaller activation energy (Scheme I).

Table II. Observed Activation Parameters of the IE formation of DPP and Activation Parameters of Solvent Viscous Flow

solvent	ΔE^*_{obsd}, kJ/mol	ΔE^*_{η}, kJ/mol	ΔV^*_{obsd}, cm^3/mol	ΔV^*_{η}, cm^3/mol
acetone	17.5	7.1	4.9	10.6–3.7
n-hexane	15.8	6.7	5.9	12.3–5.9
methylcyclohexane	18.3	10.2	9.6	19.1–13.2
ethanol	21.7	12.7	6.7	9.0–4.6
isobutyl alcohol	26.3	23.9	12.6	19.2–10.4
TMPD	31.4	24.4	24.8	37.9–27.3

Scheme I

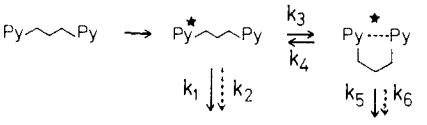

Within the framework of this scheme, we can use the following expression as a first approximation. The quantum yield ratio can be written as

$$\frac{\phi_{IE}}{\phi_{LE}} = \left(\frac{k_5}{k_1}\right)\left(\frac{k_3}{k_4 + k_5 + k_6}\right) \quad (1)$$

In a limiting case, at high viscosity or low temperature where the excimer dissociation rate becomes very slow with respect to deactivation, i.e., $k_4 \ll k_5 + k_6$, eq 1 reduces to eq 2, where k_5/k_1

$$\frac{\phi_{IE}}{\phi_{LE}} = \left(\frac{k_5}{k_1}\right)\left(\frac{k_3}{k_5 + k_6}\right) \quad (2)$$

(17) Offen, H. W. In *Organic Molecular Photophysics*; J. B. Birks, Ed.; Wiley: London, 1973; Vol. 1, p 103.
(18) Grabowski, Z. R.; Rotkiewicz, K.; Siemiarczuk, A.; Cowley, D. J.; Baumann, W. *Nouv. J. Chim.* **1979**, *3*, 443. Grabowski, Z. R.; Doblowski, J. *Pure Appl. Chem.* **1983**, *55*, 245 and references cited therein.
(19) Hara, K., to be submitted for publication.
(20) Birks, J. B. *Photophysics of Aromatic Molecules*; Wiley-Interscience: London, 1970; Chapter 7.
(21) Johnson, P. C.; Offen, H. W. *J. Chem. Phys.* **1972**, *56*, 1638. Offen, H. W.; Phillips, D. T. *J. Chem. Phys.* **1968**, *49*, 3995.

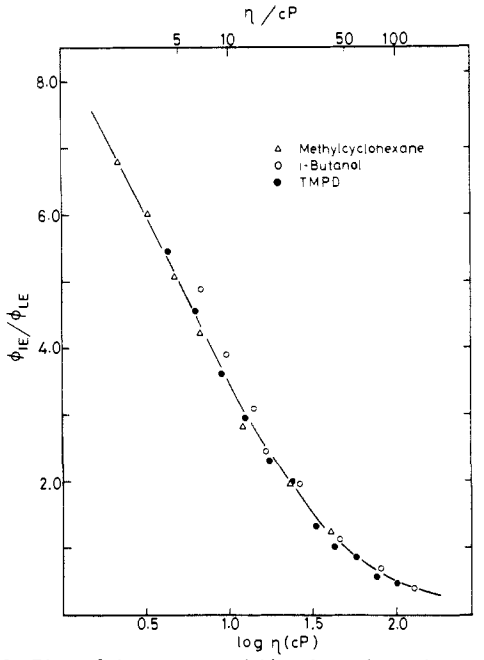

Figure 3. Plots of the quantum yield ratio against solvent viscosity η.

is expected to be independent of pressure[21] just as it is independent of solvent and temperature.[20] In addition, the lifetime of the excimer, $\tau_{IE} = 1/(k_5 + k_6)$, is not independent of pressure at all, but to a good approximation, we can regard the yield ratio ϕ_{IE}/ϕ_{LE} as being proportional to the rate constant of IE formation, k_3. The amount of the increase in τ_{IE} is supposed to be less than 10% at the pressure of 3 kbar.[7]

Pressure Effects on the IE Formation. The effect of pressure on the ratio of the quantum yields from IE state (ϕ_{IE}) and LE state (ϕ_{LE}) is presented in Figure 2. The apparent activation volumes $\Delta V^{\ddagger}_{obsd}$, given by eq 3, are obtained from the initial slopes

$$\Delta V^{\ddagger}_{obsd} = -RT\frac{\partial \ln (\phi_{IE}/\phi_{LE})}{\partial P} \qquad (3)$$

of Figure 2. Those values are listed in Table II together with the activation volumes of solvent viscous flow, $\Delta V^{\ddagger}_{\eta}$. The values of $\Delta V^{\ddagger}_{\eta}$ listed were calculated from a polynomial fit to the plots of $\ln \eta$ vs pressure. The viscosity data were obtained from the literature.[22,23] Different pressure dependence among solvents reflects that the IE formation in DPP is controlled by the viscosity change. In Figure 3, we plotted the yield ratios in *n*-hexane, isobutanol, and TMPD against their viscosities (η) for the data points for which the high-viscosity scheme is applicable. It should be noted that the rates of IE formation deduced from the quantum yield ratio are well correlated with solvent viscosity. The rates at the same viscosity are approximately equal, independent of the means by which the viscosity was produced, i.e., by changing the pressure and the solvent. For acetone the viscosity range that is in the high-viscosity scheme is so narrow that we cannot discuss it in detail. As for ethanol, there is a slight tendency to deviate from the curve in Figure 3.

When the rate constant k is expressed as shown in eq 4, where

$$k = F(\eta) \exp(-E_0/RT) \qquad (4)$$

E_0 is the intrinsic activation energy, the present universal pressure dependence indicates that the change of E_0 with solvent and pressure is small enough to be neglected for these solvents. The deviation in ethanol may occur due to the change in E_0 among solvents and with pressure. And also the change of τ_{IE} may affect it some.

Temperature Effects on the IE Formation. Figure 4 displays the Arrhenius plots of the yield ratio in various solvents. The plots

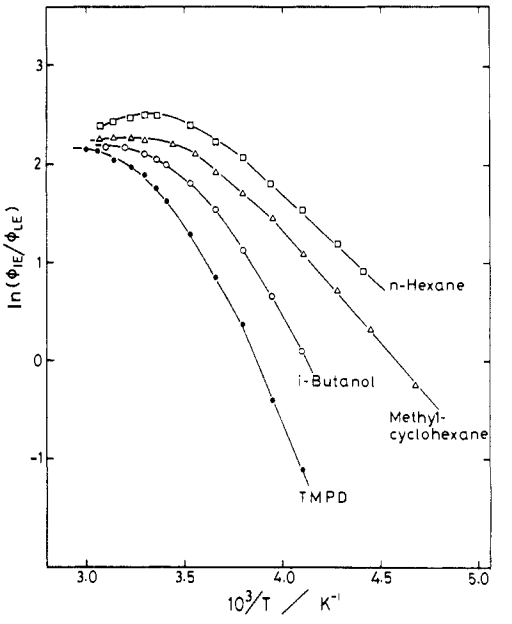

Figure 4. Arrhenius plots of the quantum yield ratio in various solvents at 1 bar.

are almost linear at temperatures less than ca. 270 K. The apparent activation energies $\Delta E^{\ddagger}_{obsd}$, expressed by eq 5, are obtained

$$\Delta E^{\ddagger}_{obsd} = -R\frac{\partial \ln (\phi_{IE}/\phi_{LE})}{\partial(1/T)} \qquad (5)$$

from the slopes of the linear region in Figure 4, which are listed in Table I together with the activation energies of solvent viscous flow $\Delta E^{\ddagger}_{\eta}$. A large value for TMPD reflects the regime of viscosity control, since the viscosity changes from 4.4 cP to 38.6 cP within our temperature range.

At the higher temperatures the data points deviate from linearity for all solvents. This deviation is due to disobedience to the high-viscosity and low-temperature condition expressed by eq 2. For another extreme condition of low viscosity or high temperature, i.e., $k_4 \gg k_5 + k_6$, eq 1 becomes eq 2′. At this limiting condition,

$$\frac{\phi_{IE}}{\phi_{LE}} = \frac{k_5 k_3}{k_1 k_4} \qquad (2')$$

the slope of $\ln (\phi_{IE}/\phi_{LE})$ vs $1/T$ gives the enthalpy of IE formation, $-\Delta H/R$, since k_3/k_4 stands for the equilibrium constant. In this region the slope becomes positive, because $\Delta H < 0$. For *n*-hexane a slight positive slope appears, but it was difficult to determine the value of ΔH accurately.

Models for the Viscosity Dependence of the IE Formation. Figure 5 displays the plots of the yield ratio against the inverse of solvent viscosity, $1/\eta$, for three solvents, i.e., methylcyclohexane, isobutanol, and TMPD. It is evident that within our viscosity range the plots have a definite curvature, implying that the simplest approach of a diffusion-controlled collision process, which is expressed as being proportional to T/η, is not applicable. Then, what type of model for describing microscopic molecular motion will most accurately reproduce the viscosity dependence of the IE formation in DPP?

There is an approach that emphasizes the volumetric requirements for viscous transport of solute molecules through solvents.[24] If this "free volume limited model" is adopted for the IE formation of DPP, then substitution for k_3 in eq 2 leads to the expression given in eq 6, where $C = (k_5/k_1)[C'/(k_5 + k_6)]$, C'

$$\phi_{IE}/\phi_{LE} = C\eta^{-\alpha} \qquad (6)$$

is a constant, and α is a parameter representing a measure of the fraction of the critical volume required for motion in the solvent. Such motion is needed for the solute to undergo some relative

(22) Thomas, M. M.; Drickamer, H. G. *J. Chem. Phys.* **1981**, *74*, 3198.
(23) Bridgman, P. W. *Collected Experimental Papers*; Harvard University: Cambridge, MA, 1964; Vol. IV.

(24) Johnson, J. E. *J. Chem. Phys.* **1975**, *63*, 4047.

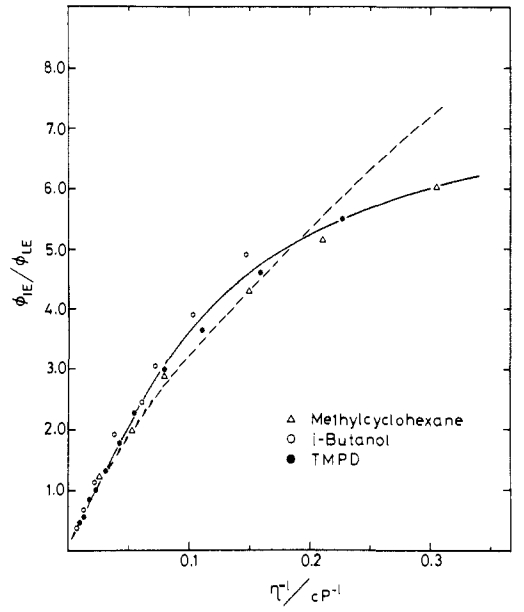

Figure 5. Plots of the quantum yield ratio against $1/\eta$. The solid line represents the best fit for the hindered rotation model based on Kramers' theory, and the dashed line represents the best fit for the free volume limited model.

motion of the two chromophore groups. The greater free volume needed for the chromophore would be expected to be reflected in a larger value of α. At first we analyzed our results in the context of this model. The dashed line in Figure 5 shows the best fit to this free volume limited model for the present data with $\alpha = 0.736$. This type of viscosity dependence with $\alpha < 1$ has been examined by other authors in different types of molecules under various conditions.[25,26] Since this α parameter is related to the volume of the chromophore moiety that must be displaced, the larger value of α for DPP could be expected naturally, as compared with 1,3-di-2-naphthylpropane (DNP) ($\alpha = 0.612$)[25] and diphenylbutadiene (DPB) ($\alpha = 0.59$).[26] In other words, this seems physically reasonable when we consider the IE formation process involves the intramolecular rotational motion of the bulky pyrenyl chromophores.

Another approach that attempts specifically to incorporate the intramolecular restrictions to rotation is the "hindered rotation model" based on Kramers' theory.[27,28] On the basis of Kramers' results, the rate of excimer formation after a single hindered rotation over a potential barrier of activation, E_0, is predicted to have the form given in eq 7, where ω_A and ω_B are the frequencies

$$k_{Kr} = \frac{\omega_A}{2\pi\omega_B}\left[\left(\frac{\beta^2}{4\mu^2} + {\omega_B}^2\right)^{1/2} - \frac{\beta}{2\mu}\right] \exp(-E_0/RT) \qquad (7)$$

corresponding to the initial potential well and the top of the barrier potential, respectively, both of which are considered to be parabolic. β is the frictional coefficient of the particle, and μ is its reduced mass. The height of the barrier is assumed to be large compared with k_BT. Applied to the present IE formation rate, eq 7 is reduced to eq 8, where $A = (k_5/k_1)[k_3/(k_5 + k_6)(r/\mu)(\omega_A/\omega_B)]$ and $B = (\mu/2\pi r)^2{\omega_B}^2$. In the course of the derivation of eq 8, a hydrodynamic assumption, that is a slipping boundary condition $\beta = 4\pi\eta r$, was adopted.

$$\frac{\phi_{IE}}{\phi_{LE}} = A[(\eta^2 + B)^{1/2} - \eta] \exp\left(-\frac{E_0}{RT}\right) \qquad (8)$$

The solid line in Figure 5 represents the best nonlinear least-squares fit of the data to this general expression for the hindered rotation model expressed by eq 8. Based on a goodness-of-fit, it is clear that the IE formation of DPP is better described by this hindered rotation model. The resultant parameters are listed in Table III. Moreover, by introducing the values of μ and r, the value of ω_B can be estimated from the obtained value of B. If we assume the effective value of r as being in between the long and short axes of the pyrene molecule, then $\omega_B = 7.6 \times 10^{13}$–$15 \times 10^{13}$ s^{-1} is obtained. This agrees with our previous result.[8]

Table III. Parameters of the Free Volume Limited Model (by eq 6) and the Hindered Rotation Model (by eq 8) for DPP

C	17.5	$A \exp(-E_0/RT)$	0.696
α	0.736	10^6B, kg^2/m^2 s^2	131
		$10^{-13}\omega_B$, s^{-1}	7.6–15

As for the solvent viscosity effects, the IE formation of DNP[25] ($\omega_B = 9.5 \times 10^{13}$ s^{-1}) and the photochemical isomerizations of *trans*-stilbene[29] ($\omega_B = 1.5 \times 10^{12}$ s^{-1}), 3,3′-diethyloxadicarbocyanine iodide (DODCI)[10] ($\omega_B = 2.5 \times 10^{13}$ s^{-1}), and DPB[30] ($\omega_B = 5.9 \times 10^{13}$ s^{-1}) have been investigated by some other authors, although this simple one-dimensional Kramers' expression has not always been fit successfully in every case. The comparatively larger value of ω_B for the IE formation of DPP implies that the potential barrier in the present case is sharper than those in the cases cited above. The key parameter is β/ω_B, which measures the strength of frictional forces impeding the passage compared with conservative forces driving down the barrier. If $\beta/\omega_B \gg 1$, then $k_{Kr} \propto \beta/\omega_B$, which is sometimes called the "Smoluchowski limit". Thus, the fact that the present case is still in the intermediate friction regime up to a considerably high viscosity range would be interpreted as originating from the large value of ω_B.

Activation Energy and Activation Volume of the IE Formation. The differentiation of eq 8 with respect to $1/T$ leads to eq 9, where

$$\frac{\partial \ln (\phi_{IE}/\phi_{LE})}{\partial(1/T)} = -\frac{E_0}{R} - \frac{\eta}{(\eta^2 + B)^{1/2}}\frac{\partial \ln \eta}{\partial(1/T)} \qquad (9)$$

$\Delta E^{\ddagger}_{\eta} = R[\partial \ln \eta/\partial(1/T)]$. Then, eq 5 is substituted into eq 9 to yield eq 10. From eq 10, by using the value of B obtained above

$$\Delta E^{\ddagger}_{obsd} = E_0 + \frac{\eta}{(\eta^2 + B)^{1/2}}\Delta E^{\ddagger}_{\eta} \qquad (10)$$

and the values of $\Delta E^{\ddagger}_{\eta}$ calculated from the Arrhenius plots of literature data of η at various temperatures, the resultant value is 14.6 kJ/mol for TMPD. It should be noted that the value of E_0 for TMPD is very close to the values of $\Delta E^{\ddagger}_{obsd}$ for *n*-hexane and acetone. This is due to the fact that for these solvents the second term of eq 10 is negligibly small because of the small viscosity values and also the small values of $\Delta E^{\ddagger}_{\eta}$. Thus, $\Delta E^{\ddagger}_{obsd}$ is almost equated with E_0. For moderately viscous solvents, i.e., ethanol and isobutyl alcohol, however, a contribution from the $\Delta E^{\ddagger}_{\eta}$ term is included. The value of 21 kJ/mol reported for DPP in toluene by Zachariasse et al.[6] may also include the contribution of $\Delta E^{\ddagger}_{\eta}$.

On the other hand, the comparatively small value of $E_0 = 8$ kJ/mol for isobutyl alcohol is obtained from a similar analysis. It is hard to explain at this stage whether this is due to specific interactions or to structure (or size) effects that are not incorporated in the theoretical description. But, since isobutanol has a chain length similar to the propyl chain, the deviation may be a result of the effect of correlated motion. An analogous size effect has been observed for the photoisomerization of *trans*-stilbene in paraffin hydrocarbons with similar chain length.[29]

Thus, it is concluded that the intrinsic activation energy of the IE formation with DPP is 15–18 kJ/mol. Since this value is equal to $E_0 = 6$–$7\ k_BT$, a requirement regarding the application of Kramers' theory is fulfilled.

As for the activation energy of the IE formation, there are some data to be compared. For the IE formation of 1,3-diphenylpropane and the excited CT formations of 3-phenyl-1-(*N*,*N*-dimethyl-

(25) Fitzgibbon, P. D.; Frank, C. W. *Macromolecules* **1981**, *14*, 1650.
(26) Velsko, S. P.; Fleming, G. R. *J. Chem. Phys.* **1982**, *76*, 3553.
(27) Kramers, H. A. *Physica (Amsterdam)* **1940**, *7*, 284.
(28) Chandrasekhar, S. *Rev. Mod. Phys.* **1943**, *15*, 1.
(29) Rothenberger, G.; Negus, D. K.; Hochstrasser, R. M. *J. Chem. Phys.* **1983**, *79*, 5360.
(30) Courtney, S. H.; Fleming, G. R. *Chem. Phys. Lett.* **1984**, *103*, 443.

amino)propane and ADMA, the reported values of activation energy are 14–23,[13] 11–13,[31] and 11 kJ/mol,[32] respectively. Therefore, the present value of 15–18 kJ/mol corresponds to the activation energy of twisting motion in the propyl group.

On the other hand, differentiating eq 8 with respect to pressure yields eq 11, where ΔV^*_0 is the intrinsic activation volume for IE

$$\frac{\partial \ln (\phi_{IE}/\phi_{LE})}{\partial P} = -\frac{\Delta V^*_0}{RT} - \frac{\eta}{(\eta^2 + B)^{1/2}} \frac{\partial \ln \eta}{\partial P} \quad (11)$$

formation. Further, eq 11 is rewritten as eq 12, where $\Delta V^*_\eta =$

$$\Delta V^*_{obsd} = \Delta V^*_0 + \frac{\eta}{(\eta^2 + B)^{1/2}} \Delta V^*_\eta \quad (12)$$

$RT\partial \ln \eta/\partial P$ is the activation volume of viscous flow. Using the value of B obtained above, we estimated the value of ΔV^*_0. At pressures of more than about 1.5 kbar, it showed a constant value of -2.5 cm^{-3}/mol for TMPD.

It is concluded that the intrinsic volume of activation for the IE formation with DPP is -2.5 cm^3/mol. As for the activation volumes of the IE formation, there are few data to be referred. However, we can say that its value is almost as comparable as the intrinsic volume change of rotational isomerization[33] and twisting isomerization.[34] And also we found that it is a few times smaller than that of intermolecular excimer formation.[35]

Concluding Remarks

We have shown that the rate of the IE formation in DPP deduced from the yield ratio is well correlated with solvent viscosity when it is studied by the high-pressure method over a wide range of viscosities (0.1–100 cP) in a continuous way with minimum specific interaction with solvent. This viscosity dependence is well described by the hindered molecular rotation model based on Kramers' expression. In terms of this model, the shape of the potential barrier was made clear. The frequency for the top of the barrier (7.6×10^{13} to 15×10^{13} s^{-1}) implies a considerably sharp barrier. The intrinsic activation parameters independent of solvent viscous flow were also determined. The intrinsic activation energy and the intrinsic activation volume of the IE formation are 15–18 kJ/mol and -2.5 cm^3/mol, respectively. These values correspond to the potential barrier of twisting motion in the propyl chain.

Registry No. 1,3-Di-1-pyrenylpropane, 61549-24-4.

(31) Van der Auweraer, M.; Gilbert, A.; De Schryver, F. C. *J. Am. Chem. Soc.* **1980**, *102*, 4007.
(32) Syage, J. A.; Felker, P. M.; Zewail, A. H. *J. Chem. Phys.* **1984**, *81*, 2233.
(33) Weale, K. E. *Chemical Reactions at High Pressures*; E. & F. N. Spon Ltd, London, 1967.
(34) Fanselow, D. L.; Drickamer, H. G. *J. Chem. Phys.* **1974**, *61*, 4567. Clark, F. T.; Drickamer, H. G. *Chem. Phys. Lett.* **1985**, *115*, 173.
(35) Förster, Th.; Leiber, C. O.; Seidel, H. P.; Weller, A. *Z. Phys. Chem. (Munich)* **1963**, *39*, 265.

Chemically Mediated Fluorescence Yield Switching in Nitroxide–Fluorophore Adducts: Optical Sensors of Radical/Redox Reactions

Neil V. Blough* and Daniel J. Simpson

Contribution from the Department of Chemistry, Woods Hole Oceanographic Institution, Woods Hole, Massachusetts 02543. *Received June 29, 1987*

Abstract: The absorption and fluorescence emission spectra and quantum yields of a series of paramagnetic nitroxide–naphthalene adducts are compared with those of diamagnetic analogues. While the absorption and emission energies of these compounds are unaffected by the presence of the nitroxyl radical substituent(s), the fluorescence quantum yields of the paramagnetic derivatives are 2.9- to 60-fold lower than the corresponding diamagnetic derivatives. Additionally, chemical reduction of the nitroxide moiety to a diamagnetic hydroxylamine produces a fluorescence yield increase that parallels nitroxyl radical loss. On the basis of this chemically mediated optical switching, compounds of this class may prove to be broadly applicable as sensitive optical probes for radicals and redox-active species in biological and chemical systems.

The ability of nitroxides to scavenge efficiently a broad array of organic and inorganic radicals has long been recognized[1,2] and employed for the detection of radicals (and some redox-active centers) in biological[3] and chemical[4] systems. The paramagnetic nitroxides are also known to be efficient quenchers of excited singlet states of aromatic hydrocarbons,[5] presumably through an intermolecular electron-exchange interaction between the ground-state nitroxide and excited-state compound within a collision complex.[5,6]

(1) Ingold, K. U. In Landolt-Börnstein *Numerical Data and Functional Relationships in Science and Technology*, Subvolume C, *Radical Reaction Rates in Liquids*; Fischer, H., Ed.; Springer-Verlag: New York, 1983; Vol. 13, pp 166–270.
(2) (a) Willson, R. L. *Trans. Faraday Soc.* **1971**, *67*, 3008–3019. (b) Nigam, S.; Asmus, K.-D.; Willson, R. L. *J. Chem. Soc., Faraday Trans. 1* **1976**, 2324–2340.
(3) (a) Melhorn, R. J.; Packer, L. *Methods Enzymol.* **1984**, *105*, 215–220. (b) Melhorn, R. J.; Packer, L. *Can. J. Chem.* **1982**, *60*, 1452–1462. (c) Quintanilha, A. T.; Packer, L. *Proc. Natl. Acad. Sci. U.S.A.* **1977**, *74*, 570–574. (d) Sarna, T.; Korytowski, W.; Sealy, R. C. *Arch. Biochem. Biophys.* **1985**, *239*, 226–233. (e) Giangrande, M.; Kevan, L. *Photochem. Photobiol.* **1981**, *33*, 721–726. (f) Leterrier, F.; Mendyk, A.; Viret, J. *Biochem. Pharmacol.* **1976**, *25*, 2469–2474. (g) Gascoyne, P. R. C.; Pethig, R.; Szent-Györgyi, A. S. *Biochim. Biophys. Acta* **1987**, *923*, 257–262. (h) Stier, A.; Sackmann, E. *Biochim. Biophys. Acta* **1973**, *311*, 400–408. (i) Rosen, G. M.; Rauckman, E. J. *Biochem. Pharmacol.* **1977**, *26*, 675–678. (j) Yamaguchi, T.; Nagatoshi, A.; Kimoto, E. *FEBS Lett.* **1985**, *192*, 259–262.
(4) (a) Blough, N. V. *Environ. Sci. Technol.* **1988**, *22*, 77–82. (b) Brownlie, I. T.; Ingold, K. U. *Can. J. Chem.* **1967**, *45*, 2427–2432. (c) Robbins, W. K.; Eastman, R. H. *J. Am. Chem. Soc.* **1970**, *92*, 6077–6079. (d) Gerlock, J. L.; Bauer, D. R. *J. Polym. Sci., Polym. Lett. Ed.* **1984**, *22*, 447–455. (e) Bosfield, W. K.; Jenkins, I. D.; Thang, S. H.; Rizzardo, E.; Soloman, D. H. *Aust. J. Chem.* **1985**, *38*, 689–698. (f) Bales, B. L.; Kevan, L. *J. Phys. Chem.* **1982**, *86*, 3836–3839. (g) Reszka, K.; Sealy, R. C. *Photochem. Photobiol.* **1984**, *39*, 293–299. (h) Hiromitsu, I.; Kevan, L. *J. Phys. Chem.* **1986**, *90*, 3088–3091. (i) Mathew, L.; Warkentin, J. *J. Am. Chem. Soc.* **1986**, *108*, 7981–7984.
(5) (a) Green, J. A.; Singer, L. A.; Parks, J. H. *J. Chem. Phys.* **1973**, *58*, 2690–2695. (b) Green, J. A.; Singer, L. A. *J. Am. Chem. Soc.* **1974**, *96*, 2730–2733. (c) Watkins, A. R. *Chem Phys. Lett.* **1974**, *29*, 526–528. (d) Kuzmin, V. A.; Tatikolov, A. S. *Chem. Phys. Lett.* **1977**, *51*, 45–47. (e) Chattopadhyay, S. K.; Das, P. K.; Hug, G. L. *J. Am. Chem. Soc.* **1983**, *105*, 6205–6210. (f) London, E. *Mol. Cell. Biochem.* **1982**, *45*, 181–188. (g) Atik, S. S.; Singer, L. A. *J. Am. Chem. Soc.* **1978**, *100*, 3234–3235. (h) Scaiano, J. C.; Paraskevopoulos, C. I. *Can. J. Chem.* **1984**, *62*, 2351–2354.

0002-7863/88/1510-1915$01.50/0